Australasian Physical & Engineering Sciences in Medicine (2019) 42:169–179
https://doi.org/10.1007/s13246-019-00727-8

SCIENTIFIC PAPER

Investigating the impact of tumour motion on TomoTherapy stereotactic ablative body radiotherapy (SABR) deliveries on 3-dimensional and 4-dimensional computed tomography

Yunfei Hu[1] · Ben Archibald-Heeren[2] · Mikel Byrne[2] · Emma Cai[3] · Yang Wang[3]

Received: 5 April 2018 / Accepted: 18 January 2019 / Published online: 21 February 2019

Abstract
TomoTherapy can provide highly accurate SABR deliveries, but currently it does not have any effective motion management techniques. Shallow breathing has been identified as one possible motion management solution on TomoTherapy, which has been made possible with the BreatheWell audiovisual biofeedback (AVB) device. Since both the shallow breathing technique and the clinical use of the BreatheWell device are novel, their implementation requires comprehensive verification and validation work. As the first stage of the validation, this paper investigates the impact of target motion on a TomoTherapy SABR delivery is assessed on both 3D CT and 4D CT using a 4D respiratory phantom. A dosimetric study on a 4D respiratory phantom was conducted, with the phantom's insert designed to move at four different amplitudes in the superior-inferior direction. SABR plans on 3D and 4D CT scans were created and measured. Critical plan statistics and measurement results were compared. It is found that for TomoTherapy SABR deliveries, by reducing the targets respiratory motion, target coverage, organ-at-risk (OAR) sparing, and delivery accuracy were improved.

Keywords TomoTherapy · Shallow breathing · Stereotactic ablative body radiotherapy

Introduction

Stereotactic ablative body radiotherapy (SABR) is a highly focused radiation therapy treatment that delivers an intense dose of radiation to a tumour while minimizing dose to the surrounding tissues in relatively few fractions. TomoTherapy (Accuray, Sunnyvale, CA, USA), as a single-modality linear accelerator, provides high accuracy for radiation therapy treatment compared to conventional linacs. Studies have suggested that TomoTherapy can provide accurate SABR delivery to different anatomical areas that are static [1–4].

However, to accurately deliver SABR to targets under respiratory motion, motion management is essential. Multiple studies reported that in the SI direction the mean lung tumour motion can range from anywhere in between 3–22 mm [5–7]. Larger motions were observed for abdominal treatment areas [8–12]. Conventional linacs can provide integrated respiratory motion management systems [13–16] for SABR treatments. Five main strategies are used to reduce respiratory motion effects: integration of respiratory movements into treatment planning, forced shallow breathing with abdominal compression, breath-hold techniques, respiratory gating techniques, and tracking techniques [17]. Although not every patient requires respiratory management methods, its use can significantly improve treatment results for NSCLC patients [18].

The current version of TomoTherapy radiation therapy planning system (RTPS) does not provide any integrated motion compensation method, such as robust optimization [19]. Additionally, it does not allow delineation on a four-dimensional (4D) CT dataset or generation of average/maximum-intensity-projection/minimum-intensity-projection based on 4D CT. Obviously this can occur in a 3rd party software, which was the method used in relevant parts this study.

✉ Yunfei Hu
Yunfei.hu@roc.team

1 Radiation Oncology Centres Gosford, 41 William St, Gosford, NSW 2250, Australia

2 Radiation Oncology Centres Wahroonga, 185 Fox Valley Rd, Wahroonga, NSW 2076, Australia

3 Icon Cancer Centre Revesby, 3/1 MacArthur Ave, Revesby, NSW 2112, Australia

There are challenges to performing gating or breath-hold treatments on TomoTherapy that include: (1) TomoTherapy treatment delivery is provided with a continuously moving couch. Upon any beam interruption the couch must be stopped and repositioned to its initial position. When the beam is resumed the couch is sent back into the treatment position in the bore. Additionally, a treatment completion procedure needs to be created and loaded. As such each beam interrupt is time consuming and can take more than 1 min. Frequent couch interruptions during treatment also increases the chance of intra-fraction motion variability and set-up error, sometimes even requiring re-imaging of the patient. Consequently, frequent beam interrupts during treatment should be avoided whenever possible; and (2) Due to its relatively low dose rate and helical delivery method, a SABR delivery on TomoTherapy can take up to 20 min. Both respiratory gating and breath-hold techniques require the beam delivery to be interrupted when the patient's breath motion is out of threshold and consequently multiple beam interruptions are expected. Consider a patient who can hold his or her breath for 30 s. For a 20 min SABR treatment delivered in breath hold this would mean 40 beam interruptions are required, possibly adding another 40–60 min to the patient's treatment. The situation is even worse for respiratory gating which requires more frequent beam interruptions. Hence the clinical implementation of respiratory gating or breath-hold techniques to SABR lung treatments is practically impossible on the current TomoTherapy system.

Tracking, as another option for motion management, requires the capability of constant online imaging during treatment delivery, which is not currently provided by TomoTherapy. TomoTherapy's binary MLC design means it can only be in either an open or a closed position, making it difficult to implement MLC tracking techniques even in the future.

Due to these difficulties, the motion management techniques mentioned above cannot be implemented on TomoTherapy. However, when treating targets with large breathing motions, motion management is essential. One potential motion management solution to TomoTherapy is the C-RAD Catalyst™ Tomo system [20], which uses a single camera to perform surface image guided radiation therapy on TomoTherapy. However, this system was not available at the author's department. Recently, another breath monitoring device, BreatheWell (Opus Medical, Sydney, NSW, Australia), was implemented at the author's department. The BreatheWell device provides audiovisual biofeedback (AVB) respiratory guidance to patients undergoing medical imaging and radiation therapy procedures [21]. It uses an infra-red (IR) projector, an IR camera and a colour camera, which together form a short range coded 3-dimensional (3D) optical imaging system to measure the patient's surface change in the anterior-posterior (AP) direction. Its functionality, accuracy and precision have been reported in detail by Pollock [22]. Further studies have reported that the use of AVB systems significantly reduced lung and abdominal intra- and inter-fractional motion as well as improved motion consistency, which is advantageous toward achieving more accurate medical imaging and radiation therapy procedures [5, 8, 23]. The BreatheWell device has been designed such that it can fit in the TomoTherapy bore, and can be used to coach the breathing of patients during treatment.

With the introduction of BreatheWell, a potential motion management solution on TomoTherapy was identified: shallow breathing. To perform shallow breathing, during simulation the patient is instructed to subjectively reduce their breathing motion (shallow breathing) [21], which is then recorded by the BreatheWell device, and converted to a threshold range. Later during treatment, this recorded threshold range is visually displayed to the patient, who then attempts to duplicate the shallow breathing motion within the range.

Both the TomoTherapy shallow breathing technique and the clinical use of the BreatheWell device are novel, with little relevant studies performed so far. Therefore, a comprehensive verification and validation study is required prior to clinical implementation. As the first stage of the study, this paper has investigated the impact of tumour motion on TomoTherapy planning and delivery, which was assessed on both 3D CT and 4D CT using a 4D respiratory phantom, to provide reference to future studies.

Materials and methods

Phantom selection and simulation

In this study, all plans and measurements were performed on the Quality Assurance System for Advanced Radiotherapy (QUASAR) respiratory motion phantom (Modus QA, London, ON, Canada) [24]. The QUASAR phantom was programmed to perform a regular sinusoidal breathing cycle with motions in the SI direction at a fixed speed of 10 Breaths Per Minute (BPM) using local control. Four sets of tests were designed, each with a different amplitude of the motion of the cylindrical insert in the SI direction. The selected motion amplitudes were ± 10 mm, ± 8 mm, ± 6 mm and ± 4 mm. Because TomoTherapy currently has no motion management techniques available, 3D CT is still commonly used for treatment planning, although more and more centres have started investigating the use of 4D CT for SABR planning [25, 26]. Therefore, in this study, for each amplitude, a 4D computed tomography (4DCT) and a conventional 3D CT were acquired.

All scans were performed on a Siemens AS Definition CT scanner with 120 kVp, a field of view (FOV) of 50 cm

and a slice thickness of 2.0 mm. An average CT based on the 4D scan was created from the scanner. As a result, for each amplitude of breathing motion, three scans were generated: the original 4D CT, the average CT created from the 4D CT, and the conventional 3D CT.

Structure delineation

The cylindrical lung insert for the QUASAR phantom was used, within which contained a sphere with a diameter of 3.0 cm and a density of water (1.0 g/cm^3). The outline of the sphere, where density was equal to or larger than 0.5 g/cm^3, was defined as the clinical target volume (CTV) for the study [shown as Structure (a) in Fig. 1]. Since each motion amplitude had three CT scans, three CTVs were generated on each CT that included: CTV 3D, delineated on the 3D CT; CTV AVG, delineated on the average CT of the 4D CT; and CTV Comp, delineated as the union of all CTVs contoured on each single phase of the 4D CT, whose sagittal views at ± 10 mm motion amplitude are shown in Fig. 2.

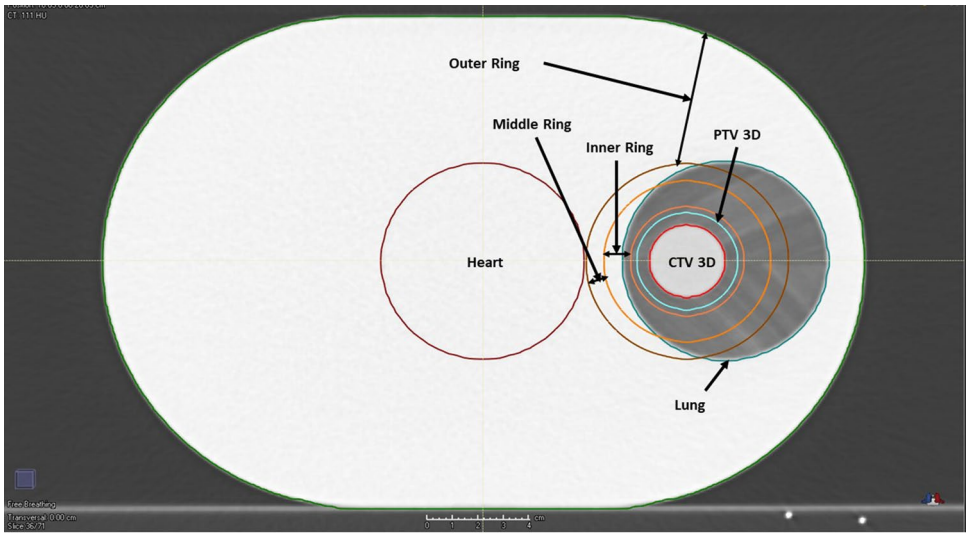

Fig. 1 Contours delineated for the ±4 mm 3D plan, including **a** CTV 3D, defined as the outline of the solid sphere in the low-density insert, where density was equal to or larger than 0.5 g/cm^3; **b** PTV 3D, defined by expanding 5 mm margin isotopically to CTV 3D; **c** Lung, defined as the outline of the cylindrical lung insert; **d** heart, defined as an 8 cm × 6 cm cylinder centred within the phantom; **e** Inner Ring, whose inner edge is 0.25 cm beyond PTV and outer edge 1.3 cm beyond PTV; **f** middle ring, whose inner edge is 1.3 cm beyond PTV and outer edge 2 cm beyond PTV; and **g** outer ring, whose inner edge is 2 cm beyond PTV and outer edge as the external of the phantom. CTV 3D: CTV contoured on 3D CT. CTV 4D: CTV contoured on averaged 4D CT. CTV Comp: CTV contoured on composite 4D CT

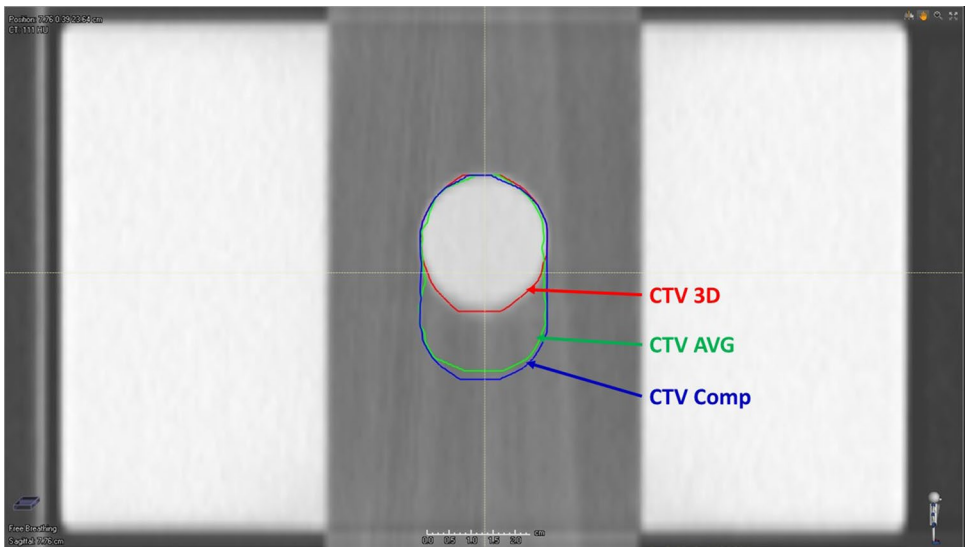

Fig. 2 Sagittal views of CTV 3D (red), CTV AVG (green) and CTV Comp (blue) when the target is moving at an amplitude of ± 10 mm

For CTV 3D, a 5 mm isotopic margin was added to generate the planning target volume (PTV) [shown as Structure (b) in Fig. 1]; for CTV AVG and CTV Comp, a smaller (3 mm) isotropic margin was added to generate PTV, because CTVs generated from these two CT scans were believed to more likely include the complete temporal information of the respiratory circle. Consequently, the PTV–CTV margin that accounts for target motion and setup uncertainty could be reduced. The assumption that when 4D CT was used, the PTV–CTV margin could be reduced is supported by previous studies [18, 27, 28].

For each motion amplitude, all CTVs and PTVs on different CTs were copied to the 3D CT. This study was a phantom study, where the only mobile subject was the target. As a result, during contour propagation, rigid registration was used to link other images to the 3D CT, with the external structure used as the guiding structure. Two OARs were created, which were: Lung [shown as Structure (c) in Fig. 1], defined as the outline of the cylindrical lung insert, and Heart [shown as Structure (d) in Fig. 1], defined as an 8 cm × 6 cm cylinder centred within the phantom. For each PTV, three rings were generated for optimization [shown as Structures (e, f) in Fig. 1]. Figures 1 and 2 show examples of the contours generated in this study.

Once contoured, the volumes of every CTV and PTV were recorded. All structure delineations were completed in RayStation version 5.0.

Planning

It was noted from the results of the "Structure delineation" section that for each motion-amplitude set, the dimensions of CTV AVG were very similar to those of CTV Comp (all Dice scores > 0.95), while the dimensions of CTV 3D were substantially different to those of CTV Comp (all Dice scores < 0.8; = 0.715, 0.690, 0.751, 0.779 for 4, 6, 8, and 10 mm, respectively). As a result, only CTV/PTV Comp and CTV/PTV 3D were used to generate plans, as a plan generated for CTV/PTV AVG was likely to create a result with negligible difference to that for CTV/PTV Comp.

Contours and 3D CT images were exported to the TomoTherapy planning system for planning. For each motion set, two sets of plans were made: plans based on the 4D CT, which was optimized with CTV/PTV Composite as the targets, and plans based on the 3D CT, with CTV/PTV 3D as the targets.

Previous studies have reported that modelling dose to a target that consists of relatively high-density tumour tissue surrounded by lower density tissue is a difficult task for treatment planning systems, and usually ends up with higher calculation uncertainties and unnecessary over-modulation of the plan [28, 29]. In this study, all optimizations were performed on the 3D CT images with structures contoured on other image sets copied across. It was thus noted that for all sets, all CTV Comp and PTV-CTV margins contained lung tissues inside, which can be problematic. In particular, for the TomoTherapy RTPS, which scales dose to meet the selected target (usually PTV) coverage, including low-density tissue in treatment volumes usually results in unnecessarily high MUs. To avoid the effect of target volumes containing low-density tissues in optimization, the hybrid density override method proposed by Wiant et al. [30] was used in this study, where for each plan the CTV's density was overridden to 1.0 g/cm^3, and the PTV–CVT margin's density was overridden to 0.8 g/cm^3. This method was previously validated at the author's department, and details of the validation are not discussed here as they are beyond the scope of this paper.

The same plan setting parameters and optimization goals were used across all plans, as shown in Table 1. Dose statistics such as target coverage, OAR dose volumes and delivery times were recorded and compared.

Plan delivery

For each measurement a piece of Gafchromic EBT3 (ISP, Wayne, NJ, United States) film was cut to the size of the cross section of the cylindrical lung insert and was placed horizontally in between the two halves of the cylindrical insert, which was then inserted into the QUASAR phantom. The QUASAR phantom was then aligned with the red laser on TomoTherapy and set to make regular motions in the SI direction with the set individual amplitude. Prior to plan delivery an MVCT was performed. After imaging, positioning of the image was checked by matching the outline of the "Lung" on the original kV CT and the acquired MVCT. The target was not used as the reference for image alignment as it was mobile and the image captured by MVCT was just a random snapshot, which could not be used to verify the phantom's position. After alignment if the required correction shift was more than 2.0 mm in any direction, the phantom was re-aligned and re-imaged. Otherwise the correction shift was applied. During the imaging process a small amount of dose was delivered to the film but this was

Table 1 Universal plan parameters applied to all plans

Delivery mode	TomoHelical
Field width	2.51 cm
Jaw mode	Dynamic
Pitch	0.287
Modulation factor	2.000
Prescription	10 Gy in 1 fractions
Structures blocked	Nil

assumed negligible compared to the plan dose and as such no correction for imaging dose was applied.

Once the phantom position was verified, plans were delivered with various motion amplitudes as described in the previous section. The Gafchromic EBT3 films were left for 24 h for full development, before scanning on an EPSON 10000XL scanner and saved as TIFF images. The green channel of the TIFF image was extracted and compared to the coronal dose map calculated by the RTPS in an in-house film analysis software. Film pixel values were converted to dose using a verified calibration curve established previously and all comparisons were conducted using absolute dose values. Point-dose comparisons and gamma analysis were performed strictly in the CTV area with both a 2% 2 mm tolerance and a 3% 3 mm tolerance. The dose threshold for the gamma analysis was 10%. Central-axis dose profiles along the motion axis (SI direction), as well as the gamma analysis results of the PTV region, were plotted. The results were then analysed qualitatively.

Results

Target volume comparison

Volumes of CTV 3D, CTV AVG and CTV Comp and their corresponding PTVs are listed below in Table 2.

From Table 2, it is found that (1) with the experimental setup, for all motion amplitudes, the CTV volumes are in the order of CTV 3D < CTV AVG < CTV Comp; (2) while the volumes of CTV 3D volume change randomly with the motion amplitude, those of CTV AVG and CTV Comp increase with increasing motion amplitude in a linear trend (R^2 values were calculated by Excel, which were 0.9963 and 0.9922 for CTV AVG and CTV Comp, respectively).

Planning statistics comparison

For each plan, target coverage, OAR dose statistics and delivery time were compared. Some important planning statistics from the Composite plans are listed below in Table 3. The same statistics from the 3D plans are listed below in Table 4. For both types of plans CTV V_{TD}, defined as the percentage volume of the CTV receiving the target dose, was calculated based on CTV Comp contoured on the 4D CT, as it would more accurately contain the target's entire temporal information during the course of treatment.

From Table 3, it is noted that CTV V_{TD} is 100% for composite plans regardless of the target motion amplitude. In addition, although the difference is very small and the trend is not completely linear, the OAR doses, as well as the delivery time, tend to increase with increasing motion amplitude ($R^2 = 0.9709$, 0.9268, and 0.9154 for Lung D_{20}, Heart average dose, and Delivery time, respectively).

From Table 4, it is noted that the CTV coverage decreases linearly with increasing motion amplitude in 3D plans ($R^2 = 0.9789$). On the other hand, similar with CTV 3D volumes, the OAR statistics and the delivery time demonstrate no clear correlation with the motion amplitude.

To better illustrate the CTV coverages of the two planning techniques used, CTV V_{TD} for the 4D CT composite plans and the 3D plans are plotted below in Fig. 3.

Plan delivery results comparison

Gamma pass rates and average point-dose differences from 10 randomly selected points within the CTV area are listed below in Table 5. Profiles along the SI axis are plotted below in Figs. 3, 4, 5, 6, 7, 8, 9 and 10.

It is found from Table 5 that the gamma analysis pass rate significantly decreases with increasing motion amplitude for

Table 2 CTV and PTV volumes of different motion amplitudes

Motion amplitude (mm)	±4	±6	±8	±10
CTV 3D (cc)	15.32	13.18	13.08	15.36
CTV AVG (cc)	18.13	20.25	22.83	24.67
CTV Comp (cc)	19.46	21.88	24.84	26.65
PTV 3D (cc)	35.58	31.73	31.59	35.66
PTV AVG (cc)	30.31	33.44	37.23	39.97
PTV Comp (cc)	32.09	35.59	39.85	42.5

Table 3 CTV and OAR statistics of composite plans

	±4 mm	±6 mm	±8 mm	±10 mm
CTV Comp				
V_{TD} (%)	100.00	100.00	100.00	100.00
Lung				
D_{20} (Gy)	6.52	6.94	7.27	7.45
Heart				
Average dose (Gy)	1.64	1.75	1.79	1.83
Delivery time (s)	460.00	479.60	545.60	554.50

Table 4 CTV and OAR statistics from the 3D plans

	±4 mm	±6 mm	±8 mm	±10 mm
CTV Comp				
V_{TD} (%)	99.49	94.50	86.33	76.26
Lung				
D_{20} (Gy)	6.78	6.36	6.53	6.84
Heart				
Average dose (Gy)	1.75	1.63	1.57	1.63
Delivery time (s)	477.8	439.4	429.3	467.2

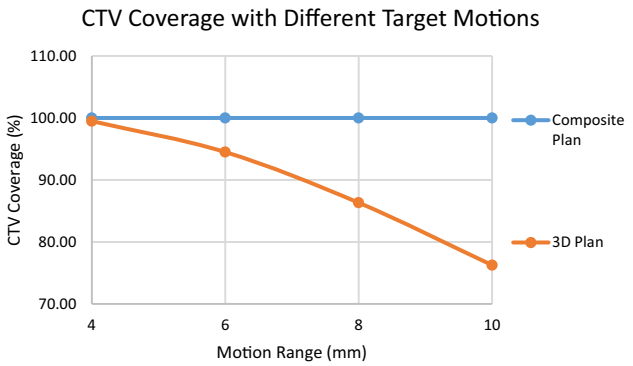

Fig. 3 Change of CTV V_{TD} with target motions for both types of plans

both plans. In addition, the gamma pass rate for the 3D plan is always smaller than that of the composite 4DCT plans.

Figures 4, 5, 6, 7, 8, 9, 10 and 11 show the measured 2-D dose profiles across the centre of the target in the direction of motion, as well as the corresponding profile computed by the RTPS. The RTPS profile was shifted so that its centre point would match that of the film profile. From these figures, it is noted that (1) for both plans, the agreement between the measured and the calculated profiles becomes substantially worse with increasing motion amplitude, especially in the shoulder region; (2) the agreement between measurement and calculation in plans based on 4D CTs is generally better than in plans based on 3D CTs; and (3) for plans based on 4D CTs, the horizontal axis of the figures (Distance of the profile) increases with increasing motion amplitude, while for plans based on 3D CTs, there is no clear correlation between these two items. Both of which are consistent with the correlations between the CTV volume and the motion amplitude of the corresponding set of plans.

The 2%2 mm gamma results for all plans are plotted below in Fig. 12.

It is noted from Fig. 12 that (1) the gamma pass rate significantly decreases with increasing motion amplitude, which is consistent with Table 5; (2) for the same motion amplitude, the gamma pass rate of plans based on 4D CT is substantially better than that of plans based on 3D CT in both the longitudinal

Table 5 Average point dose difference and gamma pass rates for all plans

Motion amplitude (mm)	Plan	Average point dose difference (%)	Gamma pass rate with 2% 2 mm (%)	Gamma Pass Rate with 3% 3 mm (%)
±4	4D composite	0.6	99.7	100
	3D	2.0	90.1	96.7
±6	4D composite	1.5	91.3	98.3
	3D	1.1	80.0	98.7
±8	4D composite	1.2	85.0	99.7
	3D	1.1	68.1	97.8
±10	4D composite	0.7	65.7	84.3
	3D	0.8	63.4	82.4

Fig. 4 Profiles of the ±4 mm 4D Composite plan

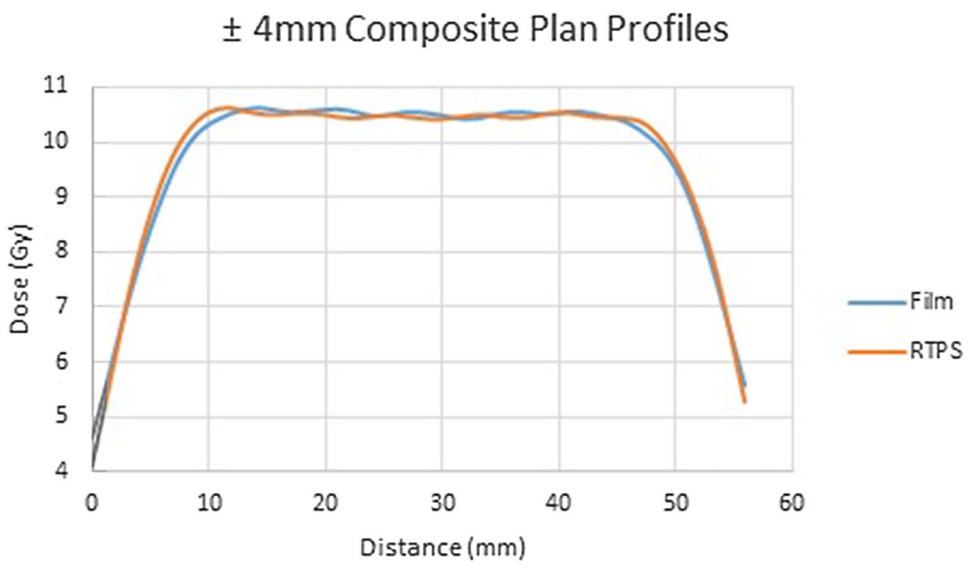

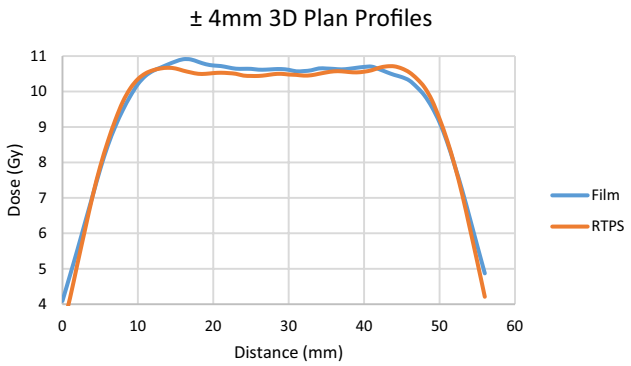

Fig. 5 Profiles of the ±4 mm 3D plan

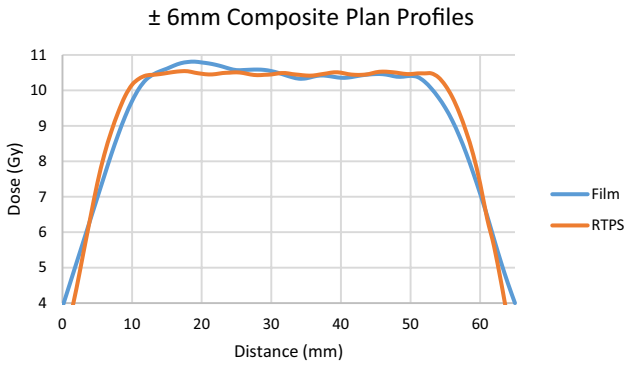

Fig. 6 Profiles of the ±6 mm 4D Composite plan

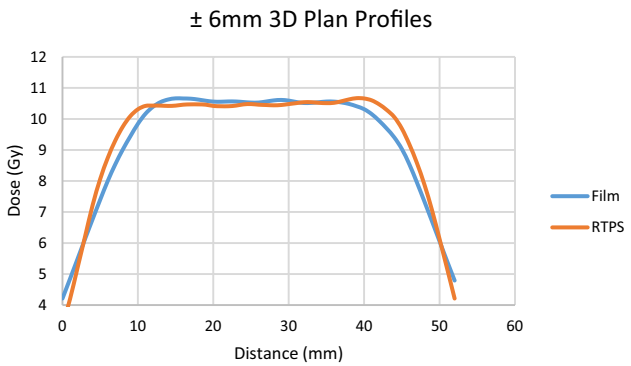

Fig. 7 Profiles of the ±6 mm 3D plan

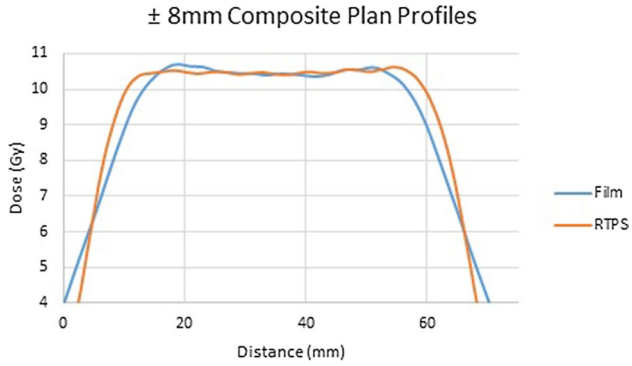

Fig. 8 Profiles of the ±8 mm 4D Composite plan

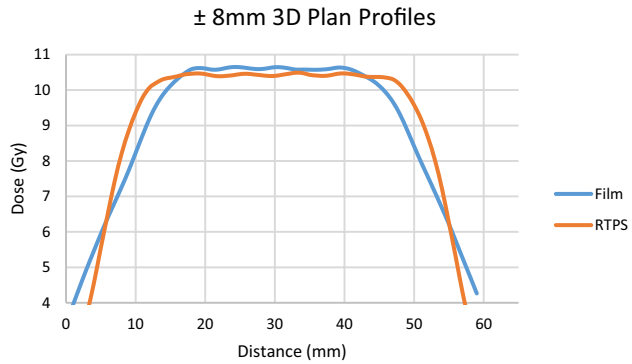

Fig. 9 Profiles of the ±8 mm 3D plan

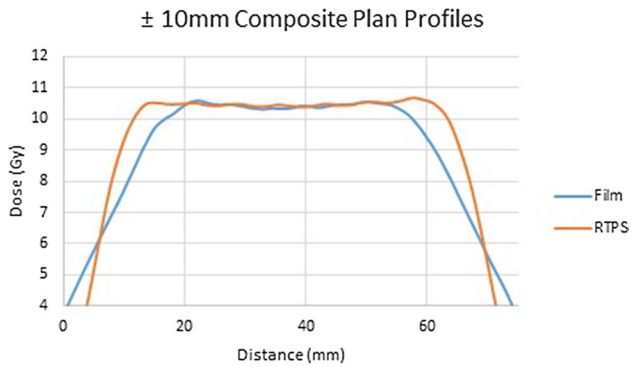

Fig. 10 Profiles of the ±10 mm 4D Composite plan

and the lateral direction; and (3) gamma analysis fails (red) mostly at the edges of the CTV region.

Discussions

This paper has investigated the impact of tumour motion on TomoTherapy SABR planning and delivery on 4D CT and 3D CT. This phantom study shows that with increasing target motion amplitude, for TomoTherapy SABR plans, OAR doses increase, and delivery accuracy worsens. The results suggest that the effect of target motion on TomoTherapy SABR planning and delivery is significant, and should be managed carefully. In this study, where the period of the breathing cycle is longer than the scan time, 3D CT in most cases cannot capture the complete target motion information, and therefore provides a worse target

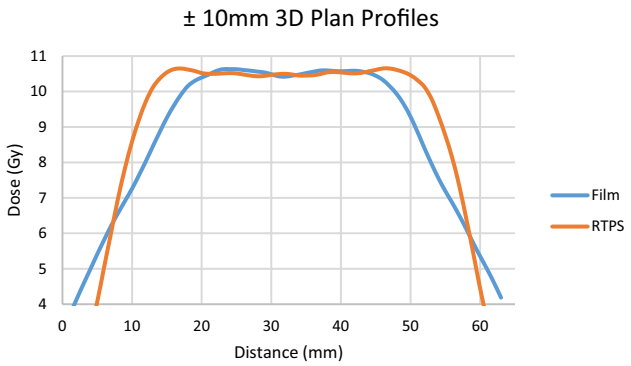

Fig. 11 Profiles of the ± 10 mm 3D plan

coverage and delivery accuracy when compared with 4D CT.

First, as shown in Table 2 and Fig. 2, in this study, with the particular experimental setup, where the period of the breathing cycle is longer than the time required to scan across the target, since the short scan time likely only captures a random snapshot of the target, the volume of CTV 3D changes randomly with increasing motion amplitude, and is always smaller than the volumes of the CTV delineated by the other two methods (Dice < 0.8 for all amplitudes). Since possible systematic shift between these volumes is minimized using scans of same parameters and rigid registration, the disagreement is mainly from the different imaging techniques. Due to this uncertainty, a large PTV–CTV is required for 3D CT scans.

Second, results from Tables 3 and 4 suggest that in this study, the planned coverage provided by the 3D plans is not acceptable, particularly for larger motions. The fact that only the ± 4 mm 3D plan provides a target coverage that is clinically acceptable (V_{TD} = 99.5% > 95.0%) is likely because the margin added to the CTV is larger than the target motion itself.

OAR statistics from Table 3 also suggest that reducing target motion reduces doses to OARs in composite plans. This can be simply explained by the fact that if the amplitude of the target motion is larger, its associated composite contour will also be larger. To deliver adequate dose to a larger target, the planning system will necessarily either escalate MU or increase treatment length, which consequently delivers larger doses to the surrounding healthy tissues. This is also supported by the observation that delivery times of plans with smaller target motions are less.

Third, results from Table 5 and Fig. 12 suggest that the plan delivery accuracy significantly worsens with increasing target motion amplitude. The most likely explanation is that radiation delivery in the presence of intra-fraction organ

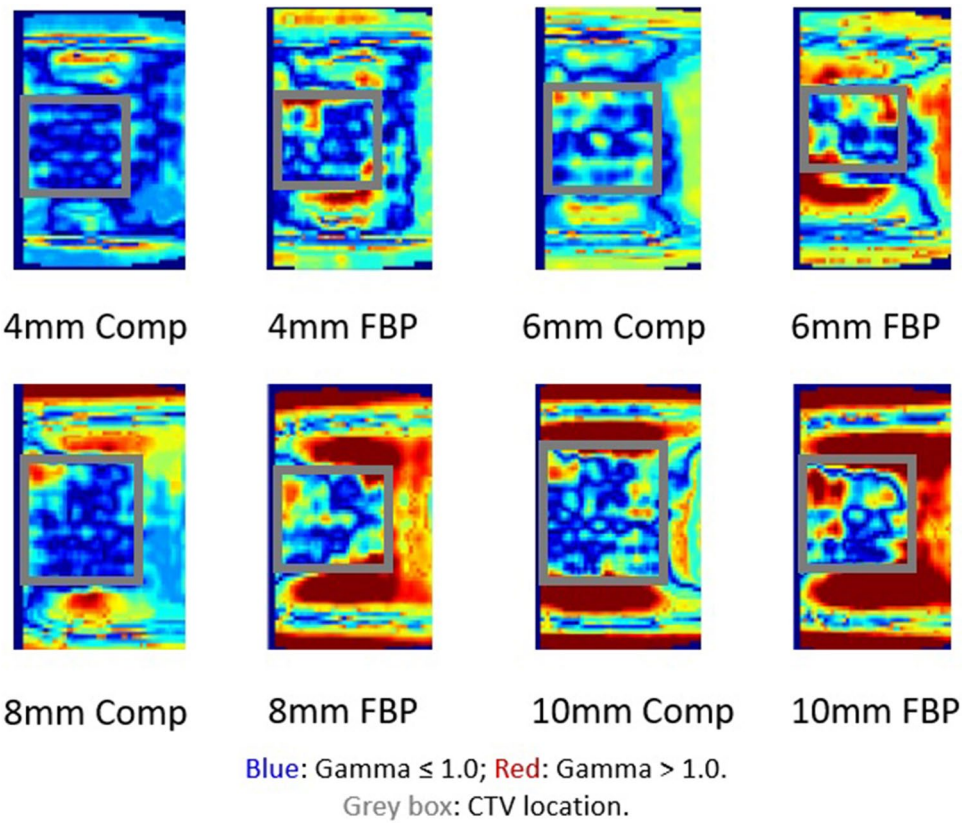

Fig. 12 2% 2 mm gamma results of all plans. The CTV area is marked by a grey box in each gamma result map

motion causes an averaging or blurring of the static dose distribution over the path of the motion [31], which may then lead to a deviation between the intended and delivered dose distributions.

The other potential contributing factor to the observed disagreement is the "interplay" effect (IE), but the contribution of this factor was considered negligible in this study. IE was first described in detail by Yu et al. [32], and is found to average out over numerous fractions [33, 34]. However, as the measurements in this study were carried out over a single fraction, averaging does not take place. It has since been shown that the conclusions of Yu, which were based on a 1 cm field with 3 cm of respiratory motion (peak to peak), a breathing rate of 4 bpm and relatively fast scan speeds of 0.5–2 cm/s, do not apply directly to TomoTherapy [35]. In TomoTherapy, the analogous parameter to scan speed is the couch travel, which typically is much slower. In their study, Kissick et al. used the range of couch speeds of 0.1–0.5 cm/s, typical of standard fractionation plans. The plans in this study were SABR plans, which required a much higher dose per fraction and consequently much slower couch speeds (fastest couch speed = 0.0152 cm/s). The breathing period in our study corresponded to just 0.9 mm of couch movement, and given the 2.5 cm field width used, the beam was able to treat each part of the patient for a maximum of approximately 164 s. The implicit assumption made during planning that the plan is delivered to all breathing phases equally appears reasonable and no IE is likely to occur. IE occurs when the period of motion of a given component is of similar magnitude to the breathing period, such that the motion of breathing and the given component become synchronised [36]. The maximum MLC open times in this study were less than 1 s with minimum gantry period of 45.4 s. In considering a breathing period of 6 s this suggests no synchronization or IE should occur. In fact, the plan parameters used in this study are almost identical to plan 6 in the study by Kanagaki et al. which found no significant IE [36]. This is also consistent with the review by Zhu [37] that concluded "In Helical TomoTherapy, dosimetric impacts of IE are not significant for typical breathing patterns and magnitudes, even when only one fraction was delivered".

In this study, as the plans were optimized to deliver a uniform dose of 10 Gy to the CTV, the gamma results fail mostly at the penumbra region where the dose gradient is sharp. However, in clinical cases, where planners would usually push for higher maximum dose within the target, there will be sharp dose gradient within the CTV as well. In this case, the gamma result failure and the profile disagreement may happen in not only the penumbra region, but also the CTV region, depending on the actual dose distribution. In Fig. 12, it is also observed that for the same motion amplitude, the gamma pass rate of plans based on 4D CT is substantially better than that of plans based on 3D CT in both the longitudinal and the lateral direction. This is because in this study, a larger PTV margin (5 mm) was applied 3D plans than that (3 mm) in composite plans, and combined with dosimetric issues when optimizing dose to low-density tissue [28], the effect of dose blurring was consequently more extensive.

It is worth mentioning that currently at the author's department, for SABR plans, a 2 mm 2% gamma analysis was used instead, with > 95% result considered a pass. If this clinical QA standard is applied, then only the ± 4 mm Composite plan will pass and be approved for clinical use. Unfortunately, current patient specific QA systems utilize phantoms that are static, meaning that delivery uncertainty introduced by motion is not included in the QA procedure and will not be picked up.

From profile measurements (Figs. 4, 5, 6, 7, 8, 9, 10, 11), it is observed that in this experiment, the delivered dose coverage is always smaller than the planned one. This difference increases with increasing motion amplitude, no matter what planning technique is used. These results are consistent with what is seen from Fig. 11, that the number of points that fail gamma rate (shown as red) increases with increasing motion. The poor match between the planned and the delivered dose distribution is again because we are comparing a dose distribution measured by a moving film with one that is statically computed, resulting in a blurring of delivered dose distribution due to motion [30] whose effect increases with increasing motion amplitude.

As mentioned earlier, since the volume of CTV 3D is substantially smaller than the volume of CTV Comp, the delivered CTV coverages provided by the 3D plans are also significantly worse. When target motion is smaller than the added margin such as in the ± 4 mm case, the CTV coverage and delivery quality are acceptable, but when target motion exceeds the added margin, an under-coverage of CTV is inevitable, due to the under-estimation of the target motion. If the period of breath cycle is shorter, the coverage of the 3D plan is likely to improve.

One advantage of TomoTherapy is that a single fraction of SABR can be divided into 2–3 sessions and delivered separately simply by adding the desired number of sessions during final calculation. This approach provides the patient with an opportunity to take a break from shallow breathing, thereby potentially reducing possible interruptions during treatment. Additionally, dividing a long SABR fraction into multiple sessions allows the operator to acquire intra-fraction images between each session, which can help improving positioning accuracy and collecting data for intra-fraction motion assessment.

Study limitations and future outlook

One limitation of this study is that all results are based on the phantom performing a regular sinusoidal waveform movement. Breathing motion within a patient will be far more complicated than what is simulated by the phantom, as tumours will move in all directions at various frequencies and amplitudes and likely in an irregular pattern. Keall et al. reported no correlation between the occurrence or magnitude of tumour motion and tumour size, location or pulmonary function for lung tumours, suggesting that tumour motion should be assessed individually prior to treatment [18]. All surrounding tissues will move as well, usually in different directions to the tumour. Additionally, for clinical patients, when the plan becomes more modulated, the effect of inter-fractional errors, such as IE, can become substantially larger [36], and sometimes can cause 4D CT to either under-estimate or over-estimate the target motion [29].

Another limitation of the study is that in this study, the target was set to move at 6 s per cycle. Therefore, a 3D CT acquisition that only takes 3–4 s to scan the entire phantom, with merely 1–2 s to scan across the target, only captures a snapshot of the CTV at some random moment. In the case where the period of the breathing cycle is rapid (approximately 1–2 s), if during scan the breathing cycle happens to align with the motion of the scan, the whole trajectory of the tumour can be captured, providing more accurate delineation information on the 3D CT. However, if the breathing cycle does not align with the motion of the scan, the tumour captured by the 3D CT can be even smaller and worse than what is reported in this study due to the rapid motion.

The third limitation is that the BreatheWell device was proposed to aid shallow breathing. However, the BreatheWell device monitors a surface surrogate rather than the actual tumour motion. The correlation between surface change and tumour motion, although briefly discussed by previous studies [18], needs further investigation.

Due to some limitations of the study, the authors have planned further studies on further investigate the effect of target motion on TomoTherapy SABR delivery, as well as how to manage the breathing motion for TomoTherapy. Stage II is to assess the clinical application of the BreatheWell device for shallow breathing by performing comprehensive functionality tests and running shallow breathing tests on healthy volunteers. Stage III is to conduct shallow breathing clinical trials on TomoTherapy SABR patients using the BreatheWell device to investigate the correlation of tumour motion and patient external surface change and further assess the potential advantages and risks of implementing this novel technique.

Conclusion

In this study, the authors found that reducing tumour motion will greatly benefit TomoTherapy SABR treatments for tumours that are mobile due to respiratory motion, as it has the potential of improved target coverage, OAR dose sparing and delivery accuracy.

Compliance with ethical standards

Ethical approval The authors declare that no ethical approval is required.

References

1. Boggs H, Feigenberg S, Walter R, Patel DWB, Wu T, Rosen L (2012) Stereotactic body radiation therapy using tomotherapy for early stage NSCLC: the utility of mid-fraction CT scans to assess intrafraction tumour motion. Int J Radiat Oncol Biol Phys 84(3S):S559–S560
2. Gallo JJ, Kaufman I, Powell R et al (2015) Single-fraction spine SBRT end-to-end testing on TomoTherapy, Vero, TrueBeam, and CyberKnife treatment platforms using a novel anthropomorphic phantom. J Appl Clin Med Phys 16(1):170–182
3. Hodge W, Tomé WA, Jaradat HA et al (2006) Feasibility report of image guided stereotactic body radiotherapy (IG-SBRT) with tomotherapy for early stage medically inoperable lung cancer using extreme hypofractionation. Acta Oncol 45(7):890–896
4. Nagai A, Shibamoto Y, Yoshida M, Inoda K, Kikuchi Y (2014) Safety and efficacy of intensity-modulated stereotactic body radiotherapy using helical tomotherapy for lung cancer and lung metastasis, Bio Med Res Int. https://doi.org/10.1155/2014/473173
5. Lee D, Greer PB, Ludbrook J et al (2016) Audiovisual biofeedback improves cine-magnetic resonance imaging measured lung tumour motion consistency. Int J Radiat Oncol Biol Phys 94(3):628–636
6. Ekberg L, Holmberg O, Wittgren L, Bjelkengren G, Landberg T (1998) What margins should be added to the clinical target volume in radiotherapy treatment planning for lung cancer? Radiother Oncol 48:71–77
7. Barnes EA, Murray BR, Robinson DM, Underwood LJ, Hanson J, Roa WH (2001) Dosimetric evaluation of lung tumour immobilization using breath hold at deep inspiration. Int J Radiat Oncol Biol Phys 50(4):1091–1098
8. Kim T, Pollock S, Lee D, O'Brien R, Keall P (2012) Audiovisual biofeedback improves diaphragm motion reproducibility in MRI. Med Phys 39(11):6921–6928
9. Davies SC, Hill AL, Holmes RB, Halliwell M, Jackson PC (1994) Ultrasound quantitation of respiratory organ motion in the upper abdomen. Br J Radiol 67(803):1096–1102
10. Suramo I, Paivansalo M, Myllyla V (1984) Cranio-caudal movements of the liver, pancreas and kidneys in respiration. Acta Radiol Diagn 25(2):129–131
11. Korin HW, Ehman RL, Riederer SJ, Felmlee JP, Grimm RC (1992) Respiratory kinematics of the upper abdominal organs: a quantitative study. Magn Reson Med 23(1):172–178
12. Wade O (1954) Movement of the thoracic cage and diaphragm in respiration. J Physio 124:193–212
13. O'Connell BF, Irvine FM, Cole AJ, Hanna GG, McGarry CK (2015) Optimizing geometric accuracy of four-dimensional

CT scans quired using the wall- and couch-mounted Varian® Real-time Position Management™ camera systems. Br J Radiol 88(1046):20140624. https://doi.org/10.1259/bjr.20140624
14. Wong JW, Sharpe MB, Jaffray DA et al (1999) The use of active breathing control (ABC) to reduce margin for breathing motion. Int J Radiat Oncol Bio Phys 44(4):911–919
15. Remouchamps VM, Letts N, Vicini FA et al (2003) Initial clinical experience with moderate deep-inspiration breath hold using an active breathing control device in the treatment of patients with left-sided breast cancer using external beam radiation therapy. Int J Radiat Oncol Bio Phys 56(3):704–715
16. Bert C, Metheany KG, Doppke K, Chen GT (2005) A phantom evaluation of a stereo-vision surface imaging system for radiotherapy patient setup. Med Phys 32(9):2753–2762
17. Giraud P, Houle A (2010) Respiratory gating for radiotherapy: main technical aspects and clinical benefits. Bull Cancer 97(7):847–856. https://doi.org/10.1684/bdc.2010.1143
18. Keall PJ, Mageras GS, Balter JM et al (2006) The management of respiratory motion in radiation oncology report of AAPM Task Group 76. Med Phys 33(10):3874–3900
19. Byrne M, Hu Y, Archibald-Heeren B (2016) Evaluation of RayStation robust optimisation for superficial target coverage with setup variation in breast IMRT. Australas Phys Eng Sci Med 39:705–716
20. C-RAD Pty Ltd. CatalystTM Tomo–Improved Positioning Workflow for TomoTherapy [BROCHURE]. https://c-rad.se/content/uploads/2015/06/A4_C-RAD_folder_TomoTherapy_pages.pdf. Accessed 14th Dec 2018
21. Opus Medical Pty Ltd. Breathe well patient information. https://breathewell.co/patient-information/. Accessed 3 Nov 2017
22. Pollock S. Translational research of audiovisual biofeedback: an investigation of respiratory-guidance in lung and liver cancer patient radiation therapy (Doctoral dissertation). Retrieved from Sydney Digital Theses Database. http://hdl.handle.net/2123/15902 . Accessed 8 Nov 2017
23. Venkat RB, Sawant A, Suh Y, George R, Keall PJ (2008) Development and preliminary evaluation of a prototype audiovisual biofeedback device incorporating a patient-specific guiding waveform. Phys Med Biol 53(11):N197–N208
24. Modus Medical Devices Inc. State-of-the-art breathing simulator using patient respiratory waveforms. https://modusqa.com/motion/phantom. Accessed 8 Nov 2017
25. Sangalli G, Passoni P, Cattaneo GM et al (2011) Planning design of locally advanced pancreatic carcinoma using 4DCT and IMRT/IGRT technologies. Acta Oncol 50:72–80
26. Kim YJ, Jang SJ, Han JB et al (2014) Motion and volume change of tumor tissue depending on patient position in liver cancer treatment with use of tomotherapy. Ann Nucl Energy 65:174–180
27. Nakamura M, Narita Y, Matsuo Y et al (2008) Geometrical differences in target volumes between slow CT and 4D CT imaging in stereotactic body radiotherapy for lung tumours in the upper and middle lobe. Med Phys 35(9):4142–4148
28. Purdie TG, Moseley DJ, Bissonnette J et al (2006) Respiration correlated cone-beam computed tomography and 4DCT for evaluating target motion in Stereotactic Lung Radiation Therapy. Acta Oncol 45(7):915–922
29. Archibald-Herren B, Byrne M, Hu Y, Cai M, Wang Y (2017) Robust optimization of VMAT for lung cancer: dosimetric implications of motion compensation techniques. J Appl Clin Med Phys 18(5):104–116
30. Wiant D, Vanderstraeten C, Maurer J, Pursley J, Terrell J, Sintay BJ (2014) On the validity of density overrides for VMAT lung SBRT planning. Med Phys 41(8):081707. https://doi.org/10.1118/1.4887778
31. Badkul R, Pokhrel D, Ramanjappa T, Jiang H, Lominska C, Wang F (2016) Measurement of dose blurring effect due to respiratory motion for lung stereotactic body radiation therapy (SBRT) using Monte Carlo based calculation algorithm. Med Phys 43(6):3592
32. Yu CX, Jaffray DA, Wong JW (1998) The effects of intra-fraction organ motion on the delivery of dynamic intensity modulation. Phys Med Biol 43:91–104
33. Bortfeld T, Jokivarsi K, Goitein M, Kung JH, Jiang SB (2002) Effects of intra-fraction motion on IMRT dose delivery: statistical analysis and simulation. Phys Med Biol 47(13):2203–2220
34. Jiang SB, Pope C, Al Jarrah KM, Kung JH, Bortfeld T, Chen GT (2003) An experimental investigation on intra-fractional organ motion effects in lung IMRT treatments. Phys Med Biol 48(12):1773–1784
35. Kissick M, Boswell S, Jeraj R, Mackie TR (2005) Confirmation, refinement, and extension of a study in intrafraction motion interplay with sliding jaw motion. Med Phys 32(7):2346–2350
36. Kanagaki B, Read PW, Molloy JA, Larner JM, Sheng K (2007) A motion phantom study on helical tomotherapy: the dosimetric impacts of delivery technique and motion. Phys Med Biol 52:243–255
37. Zhu Z, Fu X (2015) The radiation techniques of tomotherapy and intensity-modulated radiation therapy applied to lung cancer. Transl Lung Cancer Res 4(3):265–274